Correlation between Mechanical and Enzymatic Events in Contracting Skeletal Muscle Fiber†

A. Shepard and J. Borejdo*

Department of Molecular Biology and Immunology, University of North Texas, 3500 Camp Bowie Boulevard, Fort Worth, Texas 7610

Received November 10, 2003; Revised Manuscript Received January 5, 2004

ABSTRACT: The conventional hypothesis of muscle contraction postulates that the interaction between actin and myosin involves tight coupling between the power stroke and hydrolysis of ATP. However, some in vitro experiments suggested that hydrolysis of a single molecule of ATP caused multiple mechanical cycles. To test whether the tight coupling is present in contracting muscle, we simultaneously followed mechanical and enzymatic events in a small population of cross-bridges of glycerinated rabbit psoas fibers. Such small population behaves as a single cross-bridge when muscle contraction is initiated by a sudden release of caged ATP. Mechanical events were measured by changes of orientation of probes bound to the regulatory domain of myosin. Enzymatic events were simultaneously measured from the same cross-bridge population by the release of fluorescent ADP from the active site. If the conventional view were true, ADP desorption would occur simultaneously with dissociation of cross-bridges from thin filaments and would be followed by cross-bridge rebinding to thin filaments. Such sequence of events was indeed observed in contracting muscle fibers, suggesting that mechanical and enzymatic events are tightly coupled in vivo.

According to the conventional hypothesis of muscle contraction, the enzymatic chemistry and mechanics of myosin cross-bridges are tightly coupled, because hydrolysis of one molecule of ATP causes one swing of the regulatory domain (RD,[1] also referred to as lever arm) of myosin subfragment-1. This view has been challenged by some in vitro experiments that suggested that hydrolysis of one ATP molecule is responsible for multiple mechanical cycles, resulting in myosin step size being many times larger than the dimension of a cross-bridge (*1*, *2*). The absence of tight coupling between enzymatic and mechanical events was directly demonstrated by measuring both events simultaneously in a single myosin molecule in vitro (*3*).

In vitro work produced impressive results (*3*−*5*), but it is not certain that cross-bridges in functioning muscle behave like purified proteins in solution. The mechanism that may be responsible for different properties of myosins in solution versus muscle fibers is molecular crowding. Crowding influences protein solubility and conformation in solution (*6*, *7*). Molecular crowding provides a rationale for the two distinct myosin cross-bridge orientations in rigor, which were observed to form at different degrees of saturation of actin filaments with myosin subfragment-1 (*8*, *9*).

In the present work we asked whether the tight coupling exists in cross-bridges of contracting muscle fiber. Under ideal circumstances such experiments should be done on a single cross-bridge to avoid averaging of asynchronous signals from a large population of molecules. This can be done in vitro by diluting the solution of myosin, but in muscle this condition can only be approximated by collecting data from a small number (200−600) of cross-bridges, a circumstance that ensures synchrony for at least 100 ms after sudden release of ATP from a cage (*10*). In this work, we measured simultaneously mechanical and enzymatic events in the same small population of cross-bridges that were synchronized by a sudden release of caged ATP.

The mechanical events were followed by measuring orientation changes of the regulatory domain (RD) of myosin subfragment-1 (S1). S1 consists of the N-terminal, globular catalytic domain and the C-terminal, α-helical regulatory domain. Recent evidence has confirmed earlier suggestions (*11*, *12*) that the catalytic domain does not rotate during contraction, and a consensus has emerged that rotation of the regulatory domain around a pivot at Gly 699 (*13*) is responsible for the cross-bridge cycle (*14*−*20*). The present experimental design is based on the fact that polarization of fluorescence (or anisotropy) of fluorescent probes bound to the regulatory domain of myosin reflects rotations of the RD (*10*, *21*, *22*).

Enzymatic events were followed by measuring the rate of dissociation from cross-bridges of Alexa-ADP, a fluorescent analogue of ADP. Fluorescent ADP is displaced from the active site of myosin by excess of nonfluorescent ATP produced from the caged precursor by a brief UV pulse. The rate of this release is measured by the rate of increase of rotational mobility of Alexa-ADP. The rotational mobility

† Supported by NIH Grants R21CA9732 and RO1AR048622 and by Grant 000130-0008-2001 from the Texas Higher Education Coordinating Board.

* To whom correspondence should be addressed.

[1] Abbreviations: caged ATP, 5-dimethyloxy-2-nitrobenzyl-caged ATP; Alexa-ATP, adenosine 5′-triphosphate−Alexa Fluor 647 2′- (or 3′-)-*O*-(*N*-(2-aminoethyl)urethane) hexa(triethylammonium) salt; RD, the regulatory domain of myosin; CD, the catalytic domain of myosin; S1, myosin subfragment-1; RLC, regulatory light chain; Rh, 5′-(iodoacetamido)tetramethylrhodamine; Rh-RLC, RLC labeled with 5′-(iodoacetamido)tetramethylrhodamine; Alexa-myosin, myosin containing Alexa-ADP at the active site.

10.1021/bi030233d CCC: $27.50
Published on Web 02/21/2004

of a small ligand increases when it is released from a large protein (*23*, *24*). The rate of release of ADP reflects the rate of shortening of the muscle (*25*). The displacement technique was first used by Bagshaw and collaborators (*26*, *27*), who used changes of intensity of fluorescence of Cy3-EDA-ATP as a measure of ATPase of myofibrillar myosin.

The present results revealed that in vivo mechanical and enzymatic events occurred simultaneously and that the lever arm rotated once for every molecule of ATP split. This suggests that rotations of cross-bridges are tightly coupled to the chemical events at the active site.

MATERIALS AND METHODS

Chemicals and Solutions. Standard chemicals and nucleotides were from Sigma (St. Louis, MO). 5-Dimethyloxy-2-nitrobenzyl-caged ATP (DMNPE-caged ATP), adenosine 5′-triphosphate−Alexa Fluor 647 2′- (or 3′-)-*O*-(*N*-(2-aminoethyl)urethane) (Alexa-ATP), 1-(4,5-dimethoxy-2-nitrophenyl)-1,2-diaminoethane-*N*,*N*,*N*′,*N*′-tetraacetic acid (DMNP-EDTA), and 5′-(iodoacetamido)tetramethylrhodamine (IATR) were from Molecular Probes (Eugene, OR). Ca-rigor solution contained 50 mM KCl, 4 mM $MgCl_2$, 0.1 mM $CaCl_2$, 1 mM DTT, and 10 mM Tris buffer, pH 7.5. All solutions used in the photolysis experiments contained 10 mM reduced glutathione. The glycerinating solution contained 80 mM potassium acetate, 0.2 mg/mL PMSF, 2 mM mercaptoethanol, and 50% glycerol.

Preparation and Mounting of Muscle Fibers. Isolated muscle fibers were prepared from glycerinated rabbit psoas muscle bundles by dissecting single fibers in glycerinating solution and attaching the ends of the tautly stretched fiber to aluminum clips glued to the microscope coverslip. The coverslip fit into a 22 mm × 22 mm × 0.2 mm homemade perfusion temperature-controlled chamber (volume = 100 μL). Mounted fibers were thoroughly washed with Ca-rigor solution and covered with #1 coverslip.

Preparation of the Regulatory Light Chain. Rabbit myosin was prepared from back and leg muscles by the method of Tonomura et al. (*28*). Chicken skeletal RLC containing a single cysteine at position 73 (*29*) was prepared by expression of RLC in a pT7-7 plasmid in BL21(DE3) cells. The construct was a gift from Dr. S. Lowey (University of Vermont). A 1 L culture was prepared and RLC isolated as described (*30*).

Labeling of RLC. Newly purified RLC in 10 mM KP_i buffer, pH 7.5, and 2 mM DTT was dialyzed overnight at 4 °C against 50 mM KCl and 10 mM Tris-HCl, pH 7.5. RLC was incubated with a 10-fold excess of 5′-IATR for 7 h on ice in the dark. Excess IATR was removed by overnight dialysis at 4 °C against 50 mM KCl, 20 mM EDTA, 0.01 M KP_i buffer, pH 7.0 and 0.5 mM DTT. The degree of labeling was 14%.

Exchanging Myosin with Rh-RLC. Labeled RLC was exchanged into fibers as described earlier (*31*). Briefly, a fiber was mounted on the coverslip, thoroughly washed with Ca-rigor solution, and incubated with 100 μL of 35 μM RLC in 50 mM KCl, 20 mM EDTA, 0.5 mM DTT, and 10 mM KP_i, pH 7.0, for 30 min in the dark at 0 °C. The fiber was rinsed three times with 100 μL of Ca-rigor solution. Then, 50 μL of 2 mM caged ATP in Ca-rigor solution plus 10 mM glutathione was added, and the muscle was covered with a coverslip. The concentration of fluorophore incorporated into muscle was estimated by comparing the fluorescent intensity of the fiber with the intensity of a known concentration of free Rh-RLC. Fluorescence of the fiber viewed with a wide-field microscope using a 10× (NA = 0.22) objective was equal to the fluorescent intensity given by ∼2 μM free Rh-RLC. The number of myosin molecules observed by the confocal microscope is equal to this concentration multiplied by the experimental volume. The width and depth of the observational (confocal) volume are approximately equal to the diffraction limit (∼0.3 μm) of the focused laser beam. Its height is limited by the confocal aperture (1.35 Airy units) to ∼3 μm, giving the volume of ∼0.3 μm^3. There are ∼400 fluorescent myosin molecules in this volume.

Labeling of the Myosin Active Site with Alexa-ATP. A muscle fiber was incubated with 0.1−0.3 μM Alexa-ATP in Ca-rigor solution for 10 min at room temperature. Excess dye was washed out with Ca-rigor solution. The degree of incorporation of Alexa-ATP into fiber was estimated by comparing the intensity of fluorescence of a known concentration of the dye with the fluorescence of labeled fibers, as in the case of labeling with Rh-RLC. Typically, 2−3 μM myosin was labeled. There are ∼500 myosin molecules labeled with Alexa-ADP in this volume.

Functionality of Exchanged Fibers. Tension development was studied by a MKB force transducer (Scientific Instruments, Heidelberg, Germany) coupled to an analogue counter (Model 6024E; National Instruments, Austin, TX). Control (unlabeled) fibers developed 0.94 ± 0.05 mN/fiber (mean ± SEM, n = 32) maximum isometric tension. Fibers exchanged with RLC fluorescently labeled at Cys 73 developed 0.96 ± 0.03 mN/fiber tension. The lack of effect on tension is consistent with previous experiments with such fibers (*32*) and with experiments that used chicken gizzard RLC labeled at Cys 108 (*21*, *31*). Likewise, labeling the myosin active site with ATP analogues had no effect on tension induced by normal ATP. Fibers labeled with 3 μM Alexa-ATP developed 0.92 ± 0.02 mN/fiber (n = 7) of tension. Fibers stimulated with 0.2 mM Alexa-ATP developed 0.68 ± 0.14 (n = 5) mN/fiber. The ATP turnover of myofibrils stimulated by control (regular) ATP was 1.8 s^{-1}. The ATP turnover of myofibrils stimulated by Alexa-ATP was within 90% of control.

Experimental Arrangement. The instrument to measure anisotropy of fluorescence was described elsewhere (*10*, *22*). The current setup differs from the earlier one in that the laser spot is not scanned and that the 633 nm excitation and Cy5 emission filters have been added to detect fluorescent ADP. Briefly, the experimental chamber was placed on stage of the confocal microscope (Zeiss, LSM 410, Thornwood, NY). A 633 nm visible light from a He/Ne laser was selected by the line selection filter to excite Alexa-ATP. A 568 nm light from the Ar/Kr laser was selected by another line selection filter to excite Rh-RLC. The polarization of the laser beam could be rotated by a $\lambda/2$ plate and directed by the dichroic mirror onto an objective [Zeiss C-Apo, 40×, numerical aperture (NA) = 1.2, water immersion]. The UV beam of an argon laser operating at 364 and 351 nm was used to photolyze the caged nucleotide.

Photogeneration of ATP. The mounted muscle fiber was perfused with 2 mM 5-dimethyloxy-2-nitrobenzyl-caged ATP (DMNPE-caged ATP). The UV beam was focused by the

objective to a Gaussian spot with width and length equal to twice the lateral resolution of the UV beam (about 0.2 μm). The height equaled 3 μm. Approximately 3 s after the scan was begun, a shutter admitting the UV light was opened for exactly 10 ms. The energy flux through the illuminated area was 9×10^{-4} mJ/μm^2. ATP stayed in the experimental volume for ~300 μs. The amount of released ATP was enough for a single turnover of ATP.

Anisotropy of Solutions. Absorption spectra were measured in the Ca^{2+}-rigor buffer at room temperature in a Beckman DU650 absorption spectrophotometer. Fluorescence anisotropies were measured in an ISS K2 spectrofluorometer (Champaign, IL). Polarized fluorescence intensities were collected using Glan-Thompson polarizers in the excitation and emitted light paths. Excitation was vertically polarized. Experiments were done at 0 °C in the Ca^{2+}-rigor buffer. Experiments on immobilized Alexa-ATP were performed at 0 °C in 90% glycerol. All samples used in fluorescence measurements had an absorption of <0.1.

Fluorescence Intensity and Anisotropy of Fibers. Fluorescence was measured with a high aperture lens (C-Apo, 40×, NA = 1.2) using confocal microscopy. Different sensitivities of detectors were compensated by adjusting photomultiplier voltages (in our microscope, detector 2 is 18% more sensitive than detector 1). Calculations showed that a high NA of the objective causes minimal distortion to the polarized intensities (*33*).

The subscripts before and after the intensity indicate the direction of polarization of excited and emitted light relative to the axis of the muscle fiber. Perpendicular anisotropy was recorded with the $\lambda/2$ plate in place. The muscle axis was oriented horizontally on a stage of a microscope. Channels 1 and 2 recorded ${}_{\perp}I_{\perp}$ and ${}_{\perp}I_{\parallel}$, respectively. Parallel anisotropy was recorded with the $\lambda/2$ absent. Channels 1 and 2 recorded ${}_{\parallel}I_{\perp}$ and ${}_{\parallel}I_{\parallel}$, respectively. The absolute anisotropies are $r_{\perp} = (\text{ch1} - \text{ch2})/[\text{ch1} + 2(\text{ch2})]$ and $r_{\parallel} = (\text{ch2} - \text{ch1})/[\text{ch1} + 2(\text{ch2})]$.

RESULTS

Enzymatic Signal. This signal arises from the release of myosin-bound Alexa-ADP to solution. Normally, free and bound dye have different anisotropies due to differences in the rate of rotation (*23*). However, in our case it is not certain that this is so. Myosin-bound Alexa-ADP is rotationally mobile and has large residual anisotropy due to a short fluorescent lifetime.[2] Figure 1 shows excitation anisotropies of solutions of substoichiometric Alexa-ATP added to myosin. The rotationally immobilized ATP (90% glycerol at 0 °C) gave limiting anisotropies that were near their theoretical limit of 0.4 (▲), indicating that the absorption and emission dipoles of Alexa-ATP are parallel. Myosin does not rotate during the fluorescent lifetime of Alexa-ATP, yet the anisotropy of myosin−Alexa-ADP (■) (Alexa-ATP is hydrolyzed by myosin) was close to that of the free probe (●), suggesting that the bound probe has significant mobility. The free dye had somewhat lower anisotropy, indicating a further increase in rotational mobility upon dissociation from the myosin active site. Thus in fiber experiments we can expect a measurable change in steady-state anisotropy, especially that anisotropy of rigor fibers is likely to be greater (arrow) than anisotropy of myosin in solution.

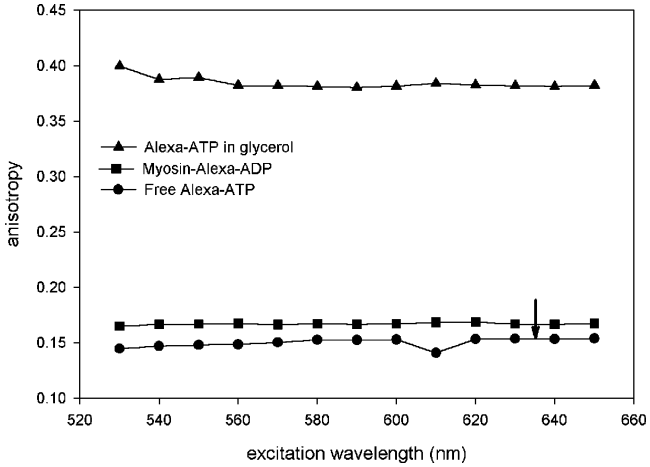

FIGURE 1: Excitation anisotropy of Alexa-ATP: Alexa-ATP immobilized in 90% glycerol at 0 °C (▲), Alexa-ADP bound to myosin at low (100 mM) ionic strength (■), and free Alexa-ATP in Ca-rigor solution at 0 °C (●). Conditions: 1 μM Alexa-ATP, 2 μM myosin heads. $\lambda_{em} = 670$ nm. Excitation slit = 2 mm, emission slit = 1 mm. The arrow indicates the observed transition. All measurements are at 0 °C.

In muscle fibers, the changes were measured by polarized intensity or anisotropy of Alexa-ATP after displacement by ATP that was rapidly photogenerated from the caged precursor. Even though the fibers were labeled with Alexa-ATP, most of the cross-bridges were in the actin−myosin−ADP state because Alexa-ATP is rapidly hydrolyzed to Alexa-ADP·P_i. P_i was removed by thorough washing with rigor solution. Figure 2 shows the appearance of muscle after incubation with Alexa-ATP. As a control, the I-bands of the same fiber were labeled with FITC−phalloidin. As expected, Alexa-ATP and FITC−phalloidin labeled the A- and I-bands, respectively. Alexa-ADP was displaced from the active site by 2 mM nonfluorescent ATP that was rapidly photogenerated from a caged precursor. Figure 3 shows the time courses of change of polarized intensity (${}_{\parallel}I_{\parallel}$ = solid line) and anisotropy ($r_{\parallel}$ = dashed line) upon generation (at the arrow) of 2 mM nonfluorescent ATP. The enzymatic signals consist of a rapid decrease corresponding to an increased rate of rotation of Alexa-ADP. Since the diffusion coefficient of free ATP is large (3.7×10^{-6} cm^2/s) (*35*), after a UV pulse there is practically no free ATP left in the experimental volume. Therefore, anisotropy, or polarized intensity, reflects irreversible displacement of bound fluorescent ADP by a single molecule of ATP. The average half-time of decay of anisotropy was 6.7 ± 1.0 ms (mean ± SEM of five experiments). The Alexa-ADP signal remains low after dissociation because release of Alexa-ADP is irreversible.

Mechanical Signal. The signal measured here is a change of steady-state anisotropy of Rh-RLC bound to the myosin cross-bridge. The transition from rigor to contraction leads to a change in steady-state anisotropy (*10*), but it is not clear whether this change is due to cross-bridge rotation or dissociation of the head from actin. To answer this question, we measured anisotropy of free, immobilized, and myosin-bound Rh-RLC in vitro. Figure 4 shows excitation anisotropies of solutions of Rh-RLC. The limiting anisotropy of the

[2] The lifetime can be calculated as ~2 ns from Perrin's equation using rotational correlation time (~2 ns) and residual anisotropy (~0.15). Those results are similar to the data of Oiwa (*34*) for related fluorescent nucleotide analogues.

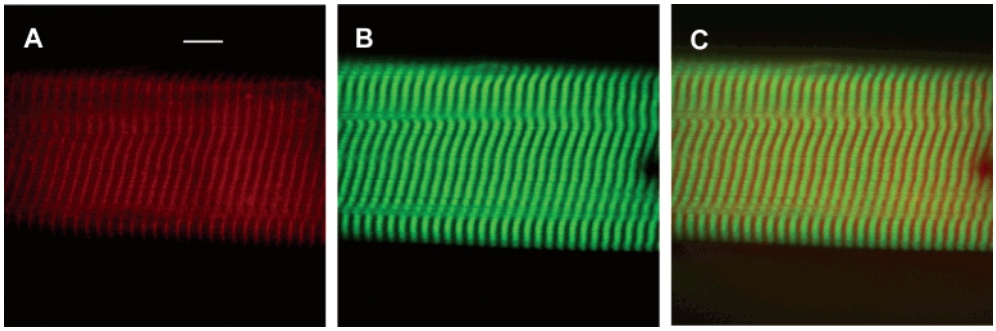

FIGURE 2: Myosin labeling with Alexa-ATP (red) and actin labeling with fluorescent phalloidin (green) in the same muscle fiber results in staining of the A- and I-bands. (A) Fiber labeled with 3 μM Alexa-ATP for 5 min at room temperature followed by a 15 min wash with Ca^{2+}-rigor solution. (B) The same fiber labeled with 0.3 μM FITC−phalloidin for $^1/_2$ h at room temperature followed by a 15 min wash with Ca^{+}-rigor solution. (C) Superposition of (A) and (B). The bar is 10 μm.

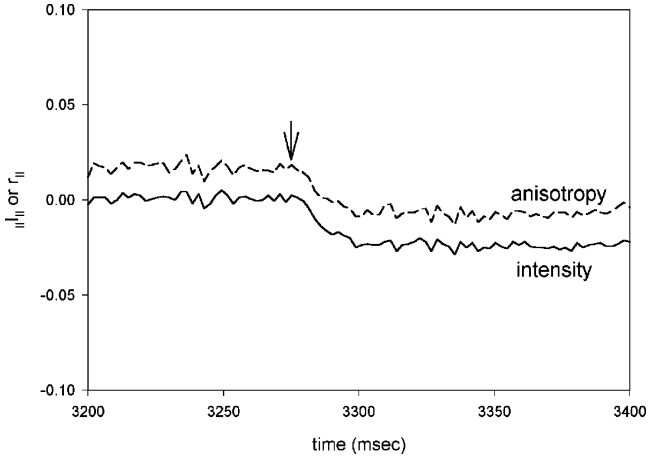

FIGURE 3: Parallel anisotropy (dashed line) and parallel polarized intensity (solid line) following ATP photogeneration (arrow) in the fiber labeled with Alexa-ATP. Signals have been corrected for photobleaching as in ref *10*; i.e., they are set to a baseline of ~0 before the pulse.

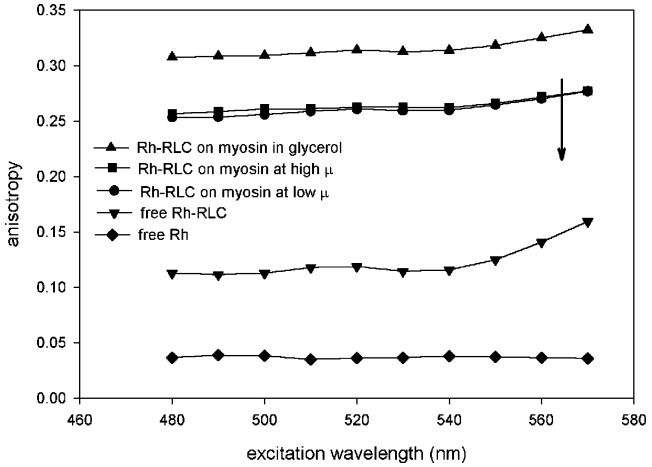

FIGURE 4: Excitation anisotropy of Rh-RLC: Rh-RLC exchanged to myosin immobilized in 90% glycerol at 0 °C (▲), Rh-RLC bound to myosin at low (100 mM) ionic strength (●) and high (0.6 M) ionic strength (■), free Rh-RLC (▼), and free rhodamine (◆). Data points for myosin in the presence of excess actin all lie between ● and ■. Conditions: 0.5 μM Rh. λ_{em} = 590 nm. Excitation slit = 2 mm, emission slit = 1 mm. The arrow indicates the observed transition. All measurements are at 0 °C.

myosin−Rh-RLC complex immobilized in 90% glycerol at 0 °C (▲) is 0.33, consistent with earlier results (*36*) and indicating that the angle between absorption and emission

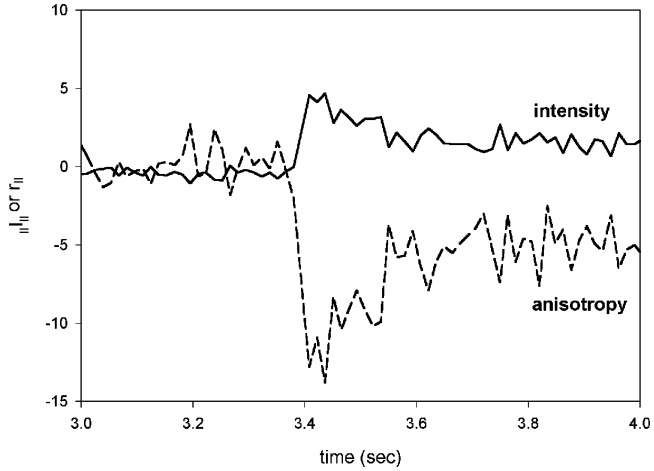

FIGURE 5: Parallel anisotropy (dashed line) and parallel polarized intensity (solid line) following ATP photogeneration (arrow) in the fiber labeled with Rh-RLC. Signals have been corrected for photobleaching.

dipoles of the probe is 19.4°. The anisotropy of myosin−Rh-RLC is decreased, indicating motion of the probe and of myosin-bound RLC. Anisotropy is the same at low (●) and high (■) ionic strength or in the presence of an excess of F-actin (data not shown), indicating that the mobility of the RD is not affected by the thick filament or actomyosin complex formation. This shows that anisotropy change observed in vivo is not due to change in the probe environment associated with myosin head detachment from thin filaments, but reflects lever arm rotation, consistent with earlier data (*29*). The anisotropy of free Rh-RLC (▼) is larger than that of free rhodamine (◆), consistent with the larger molecular weight of the complex. The change in the steady-state anisotropy that is monitored in fiber experiments (arrow) is equal to or greater than the change seen in solution because steady-state anisotropy of Alexa-ADP bound to myosin in fibers is greater.

We next measured the mechanical signal in muscle fibers by polarized intensity or anisotropy of Rh-RLC bound to RD of a cross-bridge after sudden release of ATP. The striation pattern of muscle exchanged with fluorescent RLC was very good (*10*). Figure 5 shows the time course of parallel polarized fluorescence ($_{||}I_{||}$ = solid line) and of anisotropy ($r_{||}$ = dashed line). They reflect rotation of the RD during single turnover of ATP by cross-bridges. Consistent with earlier observations (*10*, *22*), the mechanical signal consists of a rapid change reflecting rotation of RD

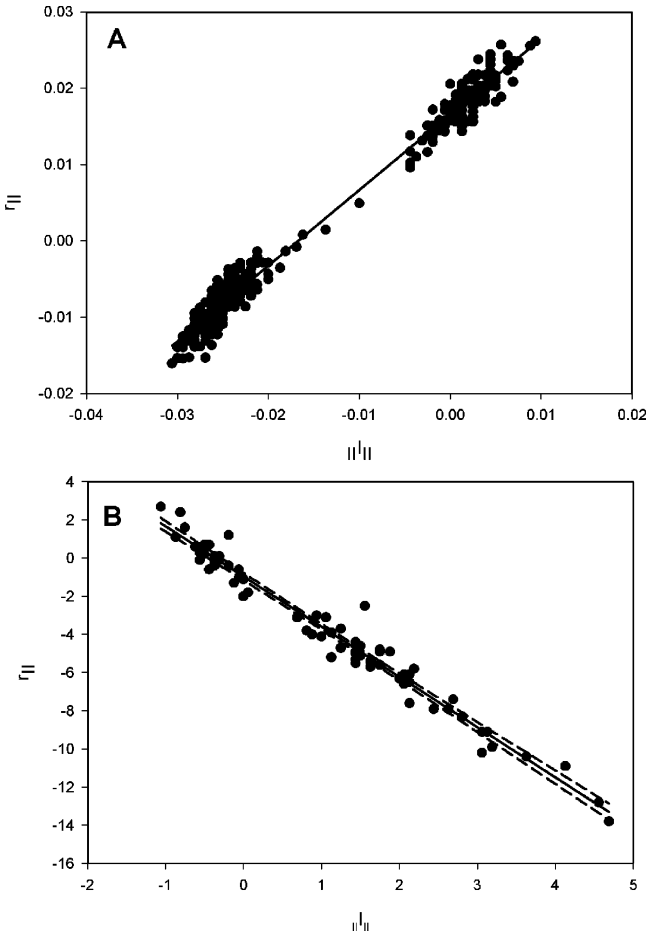

FIGURE 6: Correspondence between anisotropy and intensity signals: (A) data from Figure 4; (B) data from Figure 5. The solid lines are the linear regressions. The dashed lines in (B) indicate 95% confidence limits. In (A) they lie within the solid line.

coincident with corresponding to cross-bridge dissociation. In contrast to the Alexa-ADP signal that remains low after dissociation, this phase is followed by a slow reversal corresponding to rebinding of cross-bridges to thin filaments. The average rate of rapid change was 3.6 ± 0.5 ms and of slow change 221 ± 40 ms ($n = 5$). The difference between half-times of relaxation of Alexa-ADP and RLC signals was not statistically significant ($t = 2.0$, $P = 0.105$).

Correspondence of Changes of Polarized Intensity and Anisotropy. Anisotropy measurements require two fluorescent channels: one for each polarized intensity. It would therefore require four channels to simultaneously measure rotations of RLC and Alexa-ATP, an impossible task using a regular confocal microscope that only has three fluorescence channels. To simultaneously measure time courses of RLC and Alexa-ATP rotations, it is therefore necessary to monitor polarized intensities. However, in contrast to anisotropy, which is a ratio of polarized intensities, intensity does not compensate for changes of observational volume caused by possible muscle movement. Fortunately, in the present experiments the anisotropy and polarized intensity were closely correlated as predicted by theory (*33*); i.e., the movement artifacts were negligible. In Figure 6A every value of intensity from Figure 3 is plotted on the *X*-axis, and the corresponding value of anisotropy is plotted on the *Y*-axis. The solid line shows the linear regression, $R^2 = 0.98$. If the experimental volume changed during contraction, the correlation would not have been linear. The movement artifacts are absent because the amount of ATP generated by a short pulse of UV light in small volume is small (0.6×10^{-18} mol). Good correlation is also obtained when comparing the anisotropy and intensity of the mechanical signal (Figure 6B).

Simultaneous Measurements of Enzymatic and Mechanical Signals. Because anisotropies and polarized intensities correspond to each other, it is possible to simultaneously measure time courses of enzymatic and mechanical events in a single contraction of a small cross-bridge population of the same fiber. Figure 7A shows the confocal image of a fiber labeled with Rh-RLC. The average intensity of the bright (myosin) bands, measured by ImagePlus (Media Cybernetics, Silver Spring, MD) was ~70% larger than the intensity of dark (actin) bands. Figure 7B shows the confocal image of the same fiber labeled with Alexa-ATP. The average intensity of the bright (myosin) bands was ~75% larger than the intensity of the dark (actin) bands. The two images are combined in Figure 7C to show that both labels are colocalized in the A-band. The same result was obtained when myosin was exchanged with fluorescein-RLC. Figure 8A compares the time courses of change of mechanical and enzymatic signals. The enzymatic signal (red) has a lower S/N ratio than the corresponding mechanical signal (green) because anisotropy of Alexa-ATP changes little upon dissociation (Figure 1) as a consequence of its short fluorescence lifetime. The RLC begins to rotate at the same time that ADP is released. There is no indication of mechanical change other than the slow rebinding. The expanded time scale (Figure 8B) shows that the two signals are coincident within at least 10 ms. The same result was obtained in 11 experiments using fluorescein-labeled RLC and in 5 experiments using Rh-labeled RLC.

DISCUSSION

The present study shows that in contracting muscle the release of ADP is coincident with cross-bridge dissociation

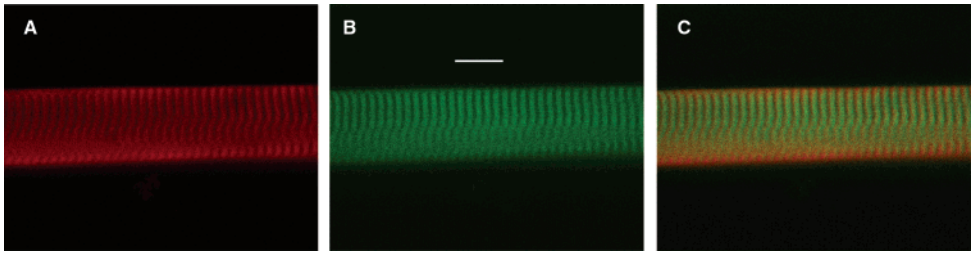

FIGURE 7: Images of a fiber labeled with Rh-RLC and viewed through an LP 590 (rhodamine) filter (A) and Alexa-ATP viewed through an LP 647 (Cy5) filter (B). The fiber labeled with Alexa is in deep red but was assigned to a green channel. (C) Superposition of (A) and (B). The scale shown in (B) is 10 μm.

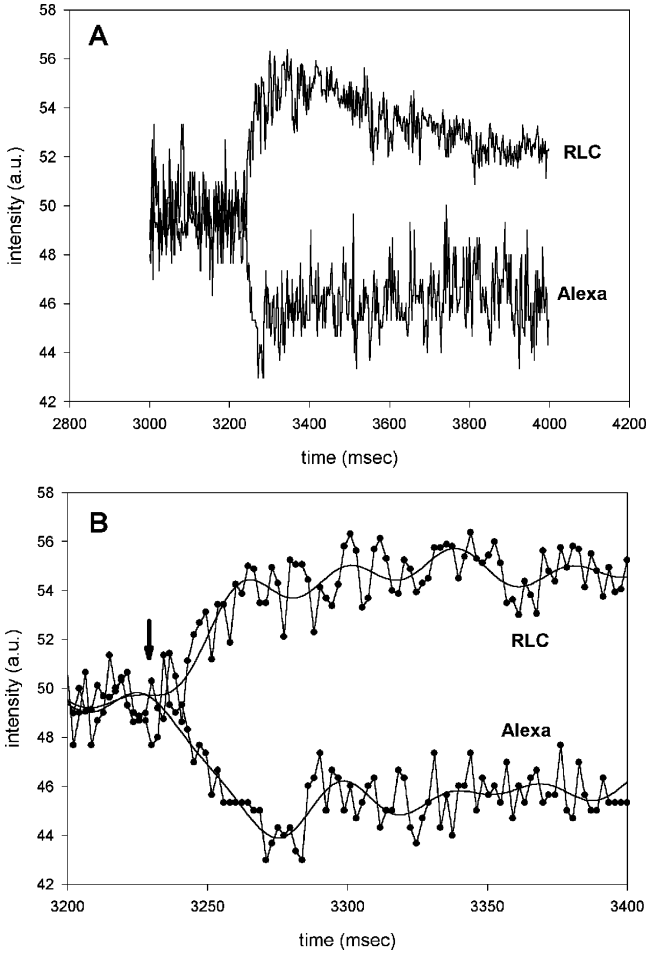

FIGURE 8: (A) Correlation between rotations of the perpendicular polarized intensity of RLC (top curve) and the parallel polarized intensity of Alexa-ATP (bottom curve). (B) The data are drawn on an expanded time scale. The time resolution is 25 μs, but to keep the data files to reasonable size, 568 data points in (A) and 87 data points in (B) were pooled together and averaged to give a time resolution of 14.2 (A) and 2.2 ms (B).

from thin filaments. This is consistent with the conventional view that hydrolysis of one ATP molecule is associated with a single mechanical cycle of cross-bridges, i.e., that mechanical and enzymatic events are tightly coupled (*37*). If they were not, cross-bridges would execute multiple reorientation cycles before dissociating from thin filaments. Figure 9A is a classical cross-bridge cycle. It begins with photocreation of ATP (black arrow) followed by dissociation, hydrolysis, rebinding in a weak state, and the power stroke. Figure 9B illustrates the time course of anisotropy changes that are expected if we observed a single cross-bridge. Photocreation of ATP (arrow) leads to an immediate release of fluorescent ADP from the catalytic site and a change of anisotropy (enz) (for clarity, the anisotropy change is shown as an increase). Simultaneously, a cross-bridge dissociates from a thin filament, which demonstrates itself as a rapid decrease of anisotropy due to the increased rate of rotation of the RD (relax). In this state a cross-bridge interacts weakly with actin. It remains in this state until ATP is hydrolyzed and P_i is released from active site. P_i dissociation marks the transition to a putative pre-power stroke state, which may be short-lived (*5*) (not shown). This transition is expected to be associated with anisotropy increase, because the cross-bridge rotation is inhibited by actin. Finally, the cross-bridge executes a power stroke, which is expected to be accompanied by further anisotropy drop to the initial rigor value. The observed sequence of events (Figure 8) is consistent with the classical view suggesting that the conventional scheme adequately represents events occurring in contracting muscle. The power stroke was not resolved, perhaps because cross-bridges were not perfectly synchronized.

The confocal microscope defines a femtoliter volume that contains only ~400 fluorescent cross-bridges. It is crucial that the population under observation be small enough to have high degree of synchrony after the flash. The synchrony induced by uncaging ATP in such a small population is high; i.e., 400 cross-bridges rotate as one for at least 100 ms after the flash (*10*). The time course of rotation of a large population of cross-bridges, on the other hand, is the time average that may obscure small time differences. Another reason for requiring a high degree of synchrony is that there are ~20000 myosin molecules in our experimental volume.

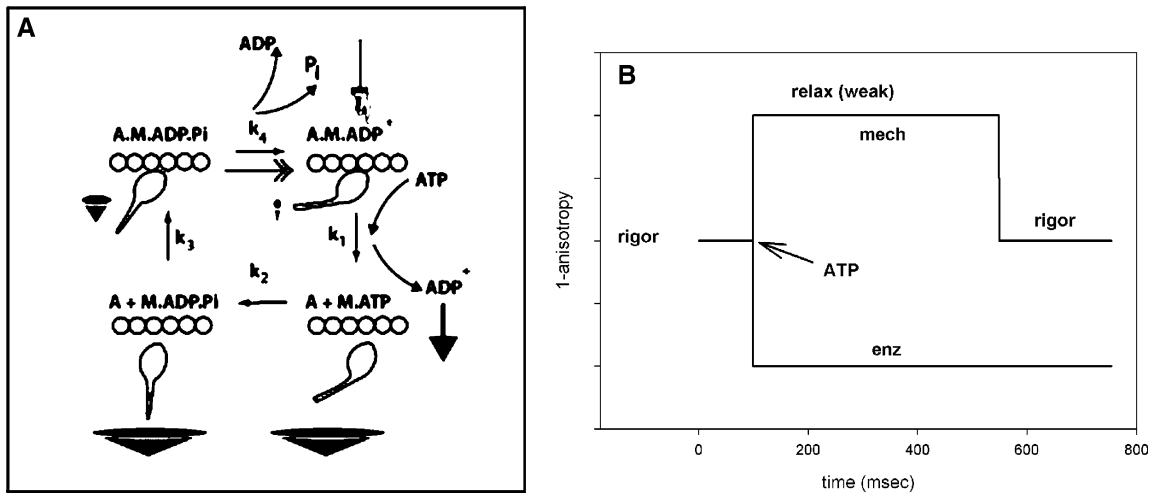

FIGURE 9: Conventional scheme of cross-bridge action. (A) The UV pulse (hand) causes release of fluorescent ADP (arrow), cross-bridge dissociation, ATP hydrolysis, cross-bridge rebinding to actin to form a weak binding state, and force generation (double-headed arrow). Fluorescent ADP is indicated by an asterisk. Cones schematically represent the extent of rotation of fluorescent dipoles on RLC. Hydrolysis of one molecule of ATP leads to a single dissociation−rebinding cycle of cross-bridges. (B) The time course of anisotropy changes expected if a single cross-bridge was observed.

Out of this population, ~400 molecules are fluorescently labeled with Rh-RLC and ~500 with Alexa-ADP. It is statistically unlikely that the same myosin molecule carries both labels. Thus while our results do not reflect events occurring at the same molecule, they reflect the behavior of a small population of well-synchronized cross-bridges.

Possible Artifacts. It is impossible that our results are due to damage of muscle by exposure to UV light. Control experiments in which there was no caged ATP gave no change in intensity or anisotropy whatsoever (data not shown). It is also unlikely that the results are due to the fact that we compared polarized intensities rather than anisotropies. We have demonstrated that in our experiments anisotropy is equivalent to polarized intensities. This is because in our experiments the amount of photogenerated ATP is too small to cause shortening of the muscle. It is enough only for a single cross-bridge turnover, which does not produce any mechanical artifacts. It is also improbable that any artifacts arise because of heating the muscle. We estimate that heating caused by the absorption of UV light by caged ATP is ~2 °C, too small to cause any damage. In addition, there are four experimental lines of evidence proving that anisotropy change is not due to a rise in temperature. First, caged EDTA (DMNP-EDTA), which has the same UV absorption as caged ATP, causes no change of anisotropy whatsoever (not shown). Second, there is no anisotropy change in fibers left for 24 h at room temperature (denatured) (data not shown). Third, fibers in EDTA-containing solution (50 mM KCl, 2 mM EDTA, 10 mM Tris, pH 7.6) do not show any polarized intensity change. Finally, fibers devoid of myosin did not give any anisotropy change upon stimulation by caged ATP (data not shown).

Kinetics of Change. The beginning phases of cross-bridge rotation and of ADP dissociation are similar because they both reflect cross-bridge detachment. The overall time courses, however, are very different (Figure 8A). The dissociation of Alexa-ADP is irreversible event; i.e., once free, Alexa-ADP never attaches to the active site again. Rotation of RLC, in contrast, is biphasic; i.e., after detachment from actin, the RD continues to rotate, reflecting cross-bridge attachment after photogenerated ATP diffuses away. The absolute values of rates of nucleotide dissociation and of orientation change measured here are smaller than reported elsewhere (*21*, *26*). This is because ours are single turnover experiments, in which the concentration of ATP is in large excess over bound ADP only for a few milliseconds after the UV pulse. Diffusion of ATP away from the experimental volume causes reattachment of cross-bridges following original detachment, creating a load which slows the contraction. The dissociation is slowed ~15 times and reattachment ~2.7 times (*10*), suggesting that the rates in isometrically contracting muscle are $k_1 = 4.2 \times 10^3\ s^{-1}$ and $k_3 = 12.2\ s^{-1}$, respectively.

The method to measure dissociation by changes of anisotropy of fluorescence was first used by Highsmith et al. (*24*). The displacement technique was first used by Bagshaw and collaborators (*26*, *27*) to measure changes in intensity of fluorescence of excess Cy3-EDA-ATP bound to myofibrillar myosin. Those experiments differ from the present ones in that myofibrils were used with a large excess of fluorescent ATP. Isolated myofibrils present an insignificant barrier to diffusion of ATP, and so the nucleotide hydrolyzed at the active site was constantly replenished by fresh ATP. The predominant intermediate was therefore actin−myosin−ADP·P_i, and the release of the fluorescent nucleotide reflected the rate of ATP hydrolysis.

In conclusion: we incorporated Alexa-ATP and fluorescent RLC into the catalytic site and lever arm of cross-bridges, respectively. We followed rotational motion of both dyes during a single turnover of ATP. Both dyes rotated as predicted by the conventional model of muscle contraction, suggesting that enzymatic and mechanical events of a cross-bridge of contacting skeletal muscle are strongly coupled. The experiments were done on ~400 cross-bridges, which were synchronized by a sudden release of caged ATP. The final test of the model must wait until enzymatic and mechanical activities of a single cross-bridge of contracting muscle can be measured.

ACKNOWLEDGMENT

We thank Dr. Irina Akopova, Mr. John Talent, and Ms. Mahalakshmi Ramani for expert technical assistance.

REFERENCES

1. Saito, K., Aoki, T., and Yanagida, T. (1994) Movement of single myosin filaments and myosin step size on an actin filament suspended in solution by a laser trap, *Biophys. J. 66*, 769−777.
2. Yanagida, T., Kitamura, K., Tanaka, H., Hikikoshi Iwane, A., and Esaki, S. (2000) Single molecule analysis of the actomyosin motor, *Curr. Opin. Cell Biol. 12*, 20−25.
3. Ishijima, A., Kojima, H., Funatsu, T., Tokunaga, M., Higuchi, H., Tanaka, H., and Yanagida, T. (1998) Simultaneous observation of individual ATPase and mechanical events by a single myosin molecule during interaction with actin, *Cell 92*, 161−171.
4. Funatsu, T., Harada, Y., Tokunaga, M., Saito, K., and Yanagida, T. (1995) Imaging of single fluorescent molecules and individual ATP turnovers by single myosin molecules in aqueous solution, *Nature 374*, 555−559.
5. Warshaw, D. M., Hayes, E., Gaffney, D., Lauzon, A. M., Wu, J., Kennedy, G., Trybus, K., Lowey, S., and Berger, C. (1998) Myosin conformational states determined by single fluorophore polarization, *Proc. Natl. Acad. Sci. U.S.A. 95*, 8034−8039.
6. Minton, A. P. (1998) Molecular crowding: analysis of effects of high concentrations of inert cosolutes on biochemical equilibria and rates in terms of volume exclusion, *Methods Enzymol. 295*, 127−149.
7. Arakawa, T., and Timasheff, S. N. (1985) Theory of protein solubility, *Methods Enzymol. 114*, 49−77.
8. Andreev, O. A., and Borejdo, J. (1991) Myosin head can bind two actin monomers, *Biochem. Biophys. Res. Commun. 177*, 350−356.
9. Andreev, O. A., Andreeva, A. L., Markin, V. S., and Borejdo, J. (1993) Two different rigor complexes of myosin subfragment-1 and actin, *Biochemistry 32*, 12046−12035.
10. Borejdo, J., and Akopova, I. (2003) Orientational changes of cross-bridges during single turnover of ATP, *Biophys. J. 84*, 2450−2459.
11. Dos Remedios, C. G., Millikan, R. G., and Morales, M. F. (1972) Polarization of tryptophan fluorescence from single striated muscle fibers. A molecular probe of contractile state, *J. Gen. Physiol. 59*, 103−120.
12. Cooke, R., Crowder, M. S., and Thomas, D. D. (1982) Orientation of spin labels attached to cross-bridges in contracting muscle fibres, *Nature 300*, 776−778.
13. Burghardt, T. P., Garamszegi, S. P., Park, S., and Ajtai, K. (1998) Tertiary structural changes in the cleft containing the ATP sensitive tryptophan and reactive thiol are consistent with pivoting of the myosin heavy chain at Gly699, *Biochemistry 37*, 8035−8047.
14. Highsmith, S., and Eden, D. (1993) Myosin-ATP chemomechanics, *Biochemistry 32*, 2455−2458.
15. Rayment, I., Rypniewski, W., Schmidt-Base, K., Smith, R., Tomchik, D. R., Benning, M. M., Winkelman, D. A., Wesenberg, G., and Holden, H. M. (1993) Three-dimensional structure of myosin subfragment-1: a molecular motor, *Science 261*, 50−58.

16. Cooke, R. (1997) Actomyosin interaction in striated muscle, *Physiol. Rev. 77*, 671−697.
17. Goldman, Y. E. (1998) Wag the tail: structural dynamics of actomyosin, *Cell 93*, 1−4.
18. Dominguez, R., Freyzon, Y., Trybus, K. M., and Cohen, C. (1998) Crystal structure of a vertebrate smooth muscle myosin motor domain and its complex with the essential light chain: visualization of the pre-power stroke state, *Cell 94*, 559−571.
19. Houdusse, A., Kalabokis, V. N., Himmel, D., Szent-Gyorgyi, A. G., and Cohen, C. (1999) Atomic structure of scallop myosin subfragment S1 complexed with MgADP: a novel conformation of the myosin head, *Cell 97*, 459−470.
20. Warshaw, D. M., Guilford, W. H., Freyzon, Y., Krementsova, E., Palmiter, K. A., Tyska, M. J., Baker, J. E., and Trybus, K. M. (2000) The light chain binding domain of expressed smooth muscle heavy meromyosin acts as a mechanical lever, *J. Biol. Chem. 275*, 37167−37172.
21. Allen, T. S.-C., Ling, N., Irving, M., and Goldman, Y. E. (1996) Orientation changes in myosin regulatory light chains following photorelease of ATP in skinned muscle fibers, *Biophys. J. 70*, 1847−1862.
22. Borejdo, J., Ushakov, D. S., and Akopova, I. (2002) The regulatory and essential light chains of myosin rotate equally during contraction of skeletal muscle, *Biophys. J. 82*, 3150−3159.
23. Pesce, A. J., Rosen, C.-G., and Pasby, T. L. (1971) in *Fluorescence Spectroscopy*, Marcel Dekker, New York.
24. Highsmith, S., Mendelson, R. A., and Morales, M. F. (1976) Affinity of myosin S-1 for F-actin, measured by time-resolved fluorescence anisotropy, *Proc. Natl. Acad. Sci. U.S.A. 73*, 133−137.
25. Weiss, S., Rossi, R., Pellegrino, M. A., Bottinelli, R., and Geeves, M. A. (2001) Differing ADP release rates from myosin heavy chain isoforms define the shortening velocity of skeletal muscle fibers, *J. Biol. Chem. 276*, 45902−45908.
26. Chaen, S., Shirakawa, I., Bagshaw, C. R., and Sugi, H. (1997) Measurement of nucleotide release kinetics in single skeletal muscle myofibrils during isometric and isovelocity contractions using fluorescence microscopy, *Biophys. J. 73*, 2033−2042.
27. Shirakawa, I., Chaen, S., Bagshaw, C. R., and Sugi, H. (2000) Measurement of nucleotide exchange rate constants in single rabbit soleus myofibrils during shortening and lengthening using a fluorescent ATP analogue, *Biophys. J. 78*, 918−926.
28. Tonomura, Y., Appel, P., and Morales, M. F. (1966) On the molecular weight of myosin. II, *Biochemistry 5*, 515−521.
29. Sabido-David, C., Hopkins, S. C., Saraswat, L. D., Lowey, S., Goldman, Y. E., and Irving, M. (1998) Orientation changes of fluorescent probes at five sites on the myosin regulatory light chain during contraction of single skeletal muscle fibres, *J. Mol. Biol. 279*, 387−402.
30. Wolff-Long, V. L., Saraswat, L. D., and Lowey, S. (1993) Cysteine mutants of light chain-2 form disulfide bonds in skeletal muscle myosin, *J. Biol. Chem. 268*, 23162−23167.
31. Ling, N., Shrimpton, C., Sleep, J., Kendrick-Jones, J., and Irving, M. (1996) Fluorescent probes of the orientation of myosin regulatory light chains in relaxed, rigor, and contracting muscle, *Biophys. J. 70*, 1836−1846.
32. Sabido-David, C., Brandmeier, B., Craik, J. S., Corrie, J. E., Trentham, D. R., and Irving, M. (1998) Steady-state fluorescence polarization studies of the orientation of myosin regulatory light chains in single skeletal muscle fibers using pure isomers of iodoacetamidotetramethylrhodamine, *Biophys. J. 74*, 3083−3092.
33. Burghardt, T. P., Cruz-Walker, A. R., Park, S., and Ajtai, K. (2001) Conformation of Myosin Interdomain Interactions During Contraction: Deductions from muscle fibers using polarized fluorescence, *Biochemistry 40*, 4821−4833.
34. Oiwa, K., Jameson, D. M., Croney, J. C., Davis, C. T., Eccleston, J. F., and Anson, M. (2003) The 2′-O- and 3′-O-Cy3-EDA-ATP-(ADP) complexes with myosin subfragment-1 are spectroscopically distinct, *Biophys. J. 84*, 634−642.
35. Hubley, M. J., Locke, B. R., and Moerland, T. S. (1996) The effects of temperature, pH, and magnesium on the diffusion coefficient of ATP in solutions of physiological ionic strength, *Biochim. Biophys. Acta 1291*, 115−121.
36. Ajtai, K., Ilich, P. J., Ringler, A., Sedarous, S. S., Toft, D. J., and Burghardt, T. P. (1992) Stereospecific reaction of muscle fiber proteins with the 5′ or 6′ isomer of (iodoacetamido)tetramethylrhodamine, *Biochemistry 31*, 12431−12440.
37. Lymn, R. W., and Taylor, E. W. (1971) Mechanism of adenosine triphosphate hydrolysis by actomyosin, *Biochemistry 10*, 4617−4624.

BI030233D